AGU PUBLICATIONS

Geophysical Research Letters

RESEARCH LETTER
10.1002/2016GL069590

Key Points:
- Halos do not make a lightning QE field detectable further away
- QE field follows an exponential decay at long distances (>100 km)
- Self-consistent model quantifies the variation of the QE field

Correspondence to:
F. J. Pérez-Invernón,
fjpi@iaa.es

Citation:
Pérez-Invernón, F. J., F. J. Gordillo-Vázquez, and A. Luque (2016), On the electrostatic field created at ground level by a halo, *Geophys. Res. Lett.*, *43*, 7215–7222, doi:10.1002/2016GL069590.

Received 13 MAY 2016
Accepted 13 JUN 2016
Accepted article online 18 JUN 2016
Published online 2 JUL 2016

On the electrostatic field created at ground level by a halo

F. J. Pérez-Invernón[1], F. J. Gordillo-Vázquez[1], and A. Luque[1]

[1] Instituto de Astrofísica de Andalucía, CSIC, Granada, Spain

Abstract We investigate the effect of halo activity on the electrostatic field measured at ground level. We use electrostatic arguments as well as self-consistent simulations to show that, due to the screening charge in the ionosphere, the distant electrostatic field created by the uncompensated charge in a thundercloud decays exponentially rather than as the third power of the distance. Furthermore, significative ionization around the lower edge of the ionosphere slightly reduces the electrostatic field at ground level. We conclude that halos do not extend the range of detectability of lightning-induced electrostatic fields.

1. Introduction

Remotely detecting lightning strokes is essential to minimize the risks involved in electrical storms and other types of severe weather. Most of the lightning detection systems currently in operation [*Cummins et al.*, 1998; *Dowden et al.*, 2002; *Betz et al.*, 2009] rely on the measurement of the radiation field emitted by the rapidly varying current pulse of the lightning discharge [*Cummins and Murphy*, 2009; *Rakov*, 2013]. On the other hand, the electrostatic field created by a net charge within the thundercloud is rarely employed for lightning detection: whereas the radiation field decays with the inverse of the distance to the source, the electrostatic field decays as the inverse of the third power of distance for intermediate distances and much faster at longer distances. Due to this faster decay it is impractical in most situations to measure the electrostatic fields at distances longer than about 100 km.

Recently, *Bennett and Harrison* [2013] reported the detection of lightning-produced electrostatic fields at distances of up to about 300 km and thus a possible violation of the cubic decay law. *Bennett* [2014] explained this observation as resulting from the extended disk of charge induced by the thundercloud charge in the lower boundary of the ionosphere. In their model this disk is associated to a halo: a well-studied diffuse light emission closely below the ionosphere created also by lightning quasi-electrostatic fields [*Barrington-Leigh et al.*, 2001; *Pasko*, 2010]. As the horizontal extension of halos reaches about 100 km, it is reasonable to claim, as *Bennett* [2014], that they extend the reach of electrostatic fields at the ground. Furthermore, because the ground-level electric field created by the charge in the ionosphere has the opposite polarity to the field created by the cloud charge, one can also argue that the electrostatic field due to a lightning discharge reverses its polarity as it is measured at increasing distance from the source. This reversal was also reported by *Bennett and Harrison* [2013].

These observations and models motivated us to investigate in greater detail the effect of halos on the electric field measured at the ground. A key element that was missing in the above explanations is that the charge induced at the bottom of the ionosphere is a self-consistent response to the electrostatic field created by the cloud charge. In other words, it is a screening charge that reduces the electric field in the conducting ionosphere. As we describe below, we found that a screening charge at the boundary of the ionosphere does not extend the range of its causative electrostatic field; rather, it always reduces the magnitude of this field. Furthermore, the orientation of the field cannot be reversed due to the presence of this screening charge.

To reach this conclusion, we first review the physics of halos and discuss how the upper atmospheric electrical activity may influence the field at the surface. Then we present electrostatic arguments of why a screening charge at the ionosphere does not enhance the distant electric field. These arguments are then applied to our main results, where we use a self-consistent, quasi-electrostatic model of the response of the ionosphere to a lightning discharge. Within a wide range of causative charge-moments, we consistently find that the charge accumulated on the ionosphere reduces the distant field at ground level relative to the raw dipolar field created by the charges in the thundercloud. We therefore conclude that halos are not responsible of the field enhancements observed by *Bennett and Harrison* [2013].

2. The Physics of Halos

Halos are a type of transient luminous events (TLEs) in the upper atmosphere, a family of light-emitting phenomena associated with lightning that were first described by *Franz et al.* [1990] and that besides halos includes sprites, elves, blue jets, and giant blue jets [*Ebert et al.*, 2010; *Pasko et al.*, 2012; *Liu et al.*, 2015b]. TLEs in the upper atmosphere (halos, sprites, and elves) owe their existence to the rarefied air density at high altitude: as electrons experience fewer collisions with air molecules, they are more readily accelerated to high energies and are thus capable of ionizing molecules or exciting them into light-emitting states. Since the lower daytime ionosphere prevents the penetration of electric fields to high altitudes, TLEs exist mostly during nighttime. In any case, the observation of daytime TLEs would be problematic because their emissions would be swamped by scattered sunlight.

Halos are one of the most frequent types of TLEs: they are diffuse, saucer-shaped light emissions at 80 km to 90 km of altitude with diameters of about 100 km that propagate downward and last about 1 ms. In a halo electrons obviously reach energies high enough to excite substantial numbers of molecules into radiating states, namely, into $N_2(B^3\Pi_g)$, which radiates in the first positive band of nitrogen. It is, however, not so clear whether they also have enough energy to cause substantial ionization. This is certainly the case when the halo initiates a sprite, as was studied by *Luque and Ebert* [2009], *Qin et al.* [2014], and *Liu et al.* [2015c]. Besides, *Kuo et al.* [2013] detected signatures of ionization in one halo not associated with a sprite. We therefore conclude that although there may be some visible halos without a substantial effect on the upper atmospheric electron density, many others do increase this density and thus the electrical conductivity below the lower edge of the ionosphere. The increase of conductivity is not necessarily simultaneous to the luminosity of the halo: as investigated by *Luque and Gordillo-Vázquez* [2012], *Liu* [2012], and *Parra-Rojas et al.* [2013], delayed electron detachment causes conductivity enhancements on timescales of 10 ms to 100 ms, long after the luminosity has decayed.

The increase of conductivity caused by an ionizing halo can also be viewed as a transient and localized lowering of the ionosphere, which according to, e.g., *Luque and Gordillo-Vázquez* [2012] and *Liu* [2012], can reach as low as 70 km of altitude. It is this descent of the ionosphere's edge that may plausibly lead to an extended horizontal range of the electrostatic field created by a lightning stroke. Note that the ionosphere is present regardless of any halo activity, and therefore, there is always some screening charge in response to an electrostatic field: it is the extension and magnitude of this charge that may be affected by the presence of a halo.

3. Electrostatics of a Halo

Let us now consider how a lower ionosphere influences the electrostatic field at ground level. It is useful to first analyze a simplified system where the charge that the stroke leaves in and around the thundercloud can be modeled as a point charge sitting between two perfectly conducting surfaces representing the ground and the lower edge of the ionosphere. Although the voltage difference between ground and ionosphere is about 250 kV [*Rycroft et al.*, 2000], we assume that our two conductors are at the same potential. This choice is mainly justified by the roughly exponential increase of the conductivity in the atmosphere for increasing altitude. This exponential profile causes the potential drop to be almost completely concentrated at low altitude, so changes around the ionosphere have a negligible effect on the electric field caused by this potential bias. In addition, in the observations by *Bennett* [2014] the DC bias was filtered out by a 1 Hz high-pass filter.

We therefore consider a point charge placed between two conducting, grounded electrodes. In the simplest geometry of this setup both conducting surfaces are plane and parallel. In that case the electric field can be calculated by summing an infinite series of image charges. For the vertical component of the electric field at ground level at a plane distance r from the thundercloud we find

$$E_z(r) = -\frac{Q}{2\pi\epsilon_0}\sum_{n=-\infty}^{\infty}\frac{h+2nL}{\left[(h+2nL)^2+r^2\right]^{3/2}}, \tag{1}$$

where Q is the total charge in the thundercloud, located at an altitude h above ground, L is the ground-ionosphere separation, and ϵ_0 is the vacuum permittivity.

We evaluate (1) numerically by truncating the infinite series. As the sum converges very slowly for large r, we extended the sum to all terms with $-10^5 < n < 10^5$. In Figure 1 we see that the ground-level electric field

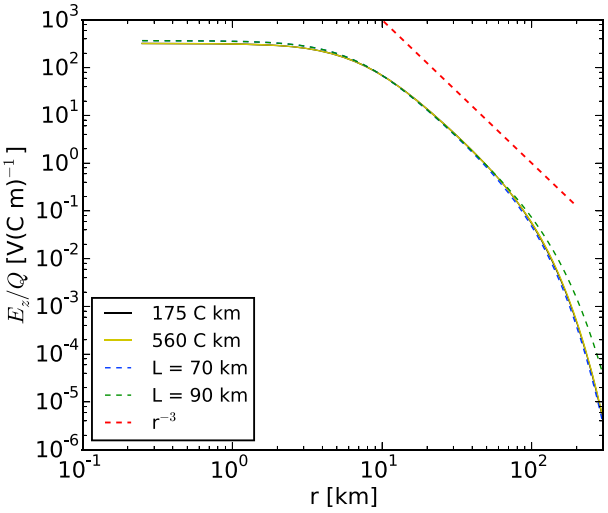

Figure 1. Vertical component of the electric field at ground level divided by its causative charge Q. We show two evaluations of (1) (dashed lines) where the ionosphere is represented by a planar, perfect conductor either at $L = 90$ km or $L = 70$ km as well as the outcome of two simulations described in section 4 (coincident solid lines). For the simulations, we plot the electric field 10 ms after the start of the discharge. We also provide an arbitrarily placed reference line to illustrate the slope of a r^{-3} decay.

$E_z(r)$ goes through three regimes as the distance to the causative lightning r increases. When $r \approx h$, the field is approximately constant; we are not interested in this range, where our simplification of the charge distribution in the cloud as a single point charge breaks down. For intermediate distances where $r \approx L \gg h$ the field decays as r^{-3} because (1) is dominated by the $n = 0$ term; in this range the field is approximately dipolar. Finally, we see that for $r \gg L$ the decay of the field is exponential and hence much faster than the dipolar field. This is a key observation, since it shows that the presence of the upper electrode induces a much faster decay of the distant field. Furthermore, we also found that as L decreases, $|E_z(r)|$ also decreases for all r, as long as $L > h$. In our context, this means that a lower ionosphere implies a lower electrostatic field at ground level.

The exponential decay of the series (1) for large r can be proven analytically by using techniques originally developed to calculate the electric field created by a crystal lattice of ions with alternating charges [see, e.g., *Borwein et al.*, 2013, p. 5ff]. This derivation fall out of the scope of this letter but, we can summarize it as follows: the Poisson summation formula transforms (1) into a series that converges much faster and can be truncated to a single term for $r \to \infty$; asymptotically, this term decays exponentially.

The exponential decay of the electric field for long distances allows us to estimate the total charge in the ionosphere, Q_i as follows. For $r \gg L$ we can view the system as the sum of two dipoles: the dipole $2Qh$ created by the causative charge and its image on the ground and the dipole $2Q_iL$ created by the charge in the halo and its image. Since at long distances there is no dipolar field, both contributions cancel:

$$Q_i = -\frac{Qh}{L}. \tag{2}$$

For our two-electrode model we can visualize the reduction of the electric field in the lower electrode caused by the upper electrode by looking at electric field lines, as shown in Figure 2a. The boundary conditions force these to be perpendicular to both conducting surfaces, and therefore, they curve outward. The upper conductor "attracts" the field lines at the expense of the line density at the lower conductor, yielding a lower field there.

Another point that can be illuminated by looking at the electric field lines is whether the screening charge in the ionosphere can reverse the orientation of the electric field at ground level. For concreteness, assume that the net charge in the thundercloud is negative. Now suppose that the electric field at some point in the lower surface points downward, thus marking the endpoint of a field line. The startpoint of this line cannot be the space charge, which is negative, nor the upper electrode, since that would imply a potential difference between the electrodes. Finally, using arguments similar to those used above, one can show that in this configuration, the radial electric field also decays exponentially, and therefore, the field line cannot extend indefinitely outward. We conclude that it is impossible for the field to point downward at the lower electrode. This means that the charge induced in the ionosphere cannot be high enough to reverse the polarity of the electric field at ground level.

There are, however, two aspects where the model of parallel conductors oversimplifies the physics of an actual halo: (1) Rather than an infinitely sharp, perfect conductor, the ionosphere consists of a smoothly

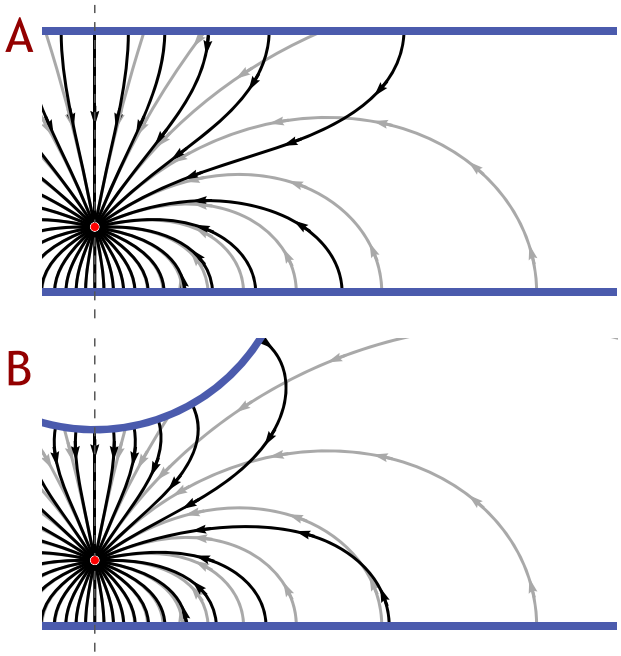

Figure 2. Field lines created by a negative point charge between two perfect conductors. (a) The field lines created by two-planar infinite are plotted as black lines. For reference we also plot the field lines created when the upper conductors in infinitely removed from the charge. We see that the upper conductor, by "attracting" field lines reduces the line density in the lower conductor. In terms of our problem, this means that a lower ionosphere reduces the electric field at the surface. (b) We consider a curved upper electrode, as would be created by a realistic halo. Here also the black lines indicate the field lines in this geometry, and the gray lines provide a reference where the upper electrode is absent. The field is enhanced directly below the vertex, but away from it the field in the lower conductor decreases.

increasing electric conductivity. (2) After a lightning stroke the ionosphere does not descend uniformly: the region directly above the stroke is ionized more intensely, and a bulge emerges from the lower edge of the ionosphere.

In the next section we will describe self-consistent simulations where these two simplifications are removed. Nevertheless, it is worth discussing qualitatively the reasons why they do not invalidate our previous argument.

1. The first issue can be quickly dismissed: a finite conductivity slows down the transport of charge to the lower boundary of the ionosphere. But we have seen that the effect of this screening charge is to decrease the electric field at ground level, so a slower charge accumulation merely implies that this decrease is weaker and slower.
2. The second issue is potentially more problematic since the curvature of the ionosphere's edge enhances the electric field directly below the point of highest curvature, which is vertically aligned with the causative lightning (see Figure 2b). However, we are interested in the electric field at locations farther than about 100 km from the parent lightning. Since this is also roughly the horizontal span of a halo, we expect that the curvature effect at those distances is negligible or even reversed, actually weakening the electric field. However, we cannot exclude that the distant electric field is enhanced by other sources of ionization away from the causating lightning, such as inhomogeneities caused by gravity waves [*Liu et al.*, 2015a] or the electromagnetic pulse (EMP) emitted by the lightning stroke.

4. Self-Consistent Simulations

Let us now flesh out the above arguments with realistic, self-consistent simulations. We use a cylindrically symmetrical density model for electron transport in the mesosphere and lower ionosphere, similar to previous models by, e.g., *Luque and Ebert* [2009], *Neubert et al.* [2011], *Liu et al.* [2015a], and *Qin et al.* [2014] (this type of models were reviewed by, e.g., *Pasko* [2010] and *Luque and Ebert* [2012]). In our model, electrons drift in a

self-consistent electric field and interact with neutrals within a minimal chemical scheme that includes impact ionization, dissociative attachment, and associative detachment:

$$e + N_2 \longrightarrow {N_2}^+ + 2e\,, \tag{3a}$$

$$e + O_2 \longrightarrow {O_2}^+ + 2e\,, \tag{3b}$$

$$e + O_2 \longrightarrow O + O^-\,, \tag{3c}$$

$$O^- + N_2 \longrightarrow N_2O + e\,. \tag{3d}$$

The electron mobility and the reaction rates for (3a)–(3c) are obtained from the solution of a steady state Boltzmann equation using BOLSIG+ [*Hagelaar and Pitchford*, 2005], with the cross sections from *Phelps and Pitchford* [1985] and *Lawton and Phelps* [1978]. For (3d) we use the fit of the data from *Rayment and Moruzzi* [1978] provided by *Luque and Gordillo-Vázquez* [2012]. The simulation domain is a cylinder that extends vertically from the ground to an altitude of 100 km and radially to 700 km, and we use an uniform cartesian grid with cell sizes $\Delta r = 500$ m, $\Delta z = 100$ m.

The charge Q in the thundercloud is modeled as a sphere of radius 0.5 km located in the central axis of our domain at an altitude $h = 7$ km [*Maggio et al.*, 2009]. We simulate the lightning stroke by varying this charge in time as

$$\frac{dQ}{dt} = I(t) = \frac{Q_{max}}{\tau_1 - \tau_2}\left(\exp(-t/\tau_1) - \exp(-t/\tau_2)\right), \tag{4}$$

where Q_{max} is the total charge lowered to the ground and τ_1 and τ_2 are, respectively, the total discharge time and the rise time of the discharge current, which we take to be $\tau_1 = 1$ ms and $\tau_2 = 0.1$ ms. The product hQ_{max}, called charge moment change, determines to a good approximation the electric field imposed on the ionosphere.

We took the air density profile from the U.S. Standard Atmosphere [*United States Committee on Extension to the Standard Atmosphere*, 1976], and our initial electron density follows *Hu et al.* [2007]. The electrons are balanced by positive ions (about 21% O_2^+ and 79% N_2^+) to ensure that we start from a neutral charge density.

Weak discharges, with charge moment hQ_{max} below ~350 C km do not cause significant ionization in the ionosphere. Hence, to study the effect of ionization in the upper atmosphere on the ground-level electric field, we consider two relevant cases: a weak discharge where the ionosphere is mostly undisturbed and a strong discharge, where there is significant ionization. We take $Q_{max} = 25$ C ($hQ_{max} = 175$ C km) for the weak discharge and $Q_{max} = 80$ C ($hQ_{max} = 560$ C km) for the strong one.

In Figures 3a and 3b we plot the space charge density induced in the lower ionosphere by each of the two discharges. For the weak discharge, we see a layer of negative charge around 70 km of altitude, which marks the effective altitude of the ionosphere for this case. The strong discharge creates a bulge in the ionosphere that descends to about 70 km within 30 km from the axis containing the causative discharge. Integrating the space charge, we find that the accumulated charge in the lower ionosphere is $Q_i = -2.56$ C for the weak discharge and $Q_i = -8.15$ C for the strong discharge, in good agreement with equation (2) with $L \approx 70$ km.

In Figure 1 we plot the simulated electric field at ground level divided by the total charge lowered to the ground. We see that the curve is close to that predicted by the analytical expression (1) for $L = 70$ km. The collapse of the two simulation profiles in Figure 1 indicates that to a good approximation, our results are linear with the driving charge Q_{max}. However, there are some factors that break this linearity:

1. *The dependence of the electron mobility with the electric field*. Since electrons are more mobile for low fields, the dielectric relaxation of the ionosphere is somewhat faster if the perturbing field is weaker. As we argued above, the relaxation of the ionosphere reduces the ground electric field, so we expect this factor to reduce the ratio E/Q_{max} for weak discharges.

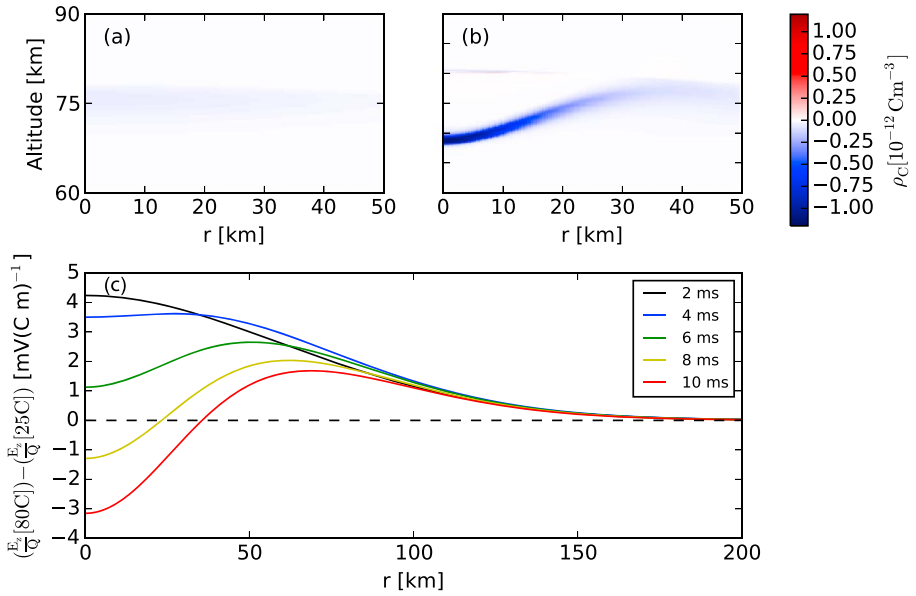

Figure 3. We can see the space density induced in the lower ionosphere by the thundercloud charge Q_{max} by (a) a weak discharge of $hQ_{max} = 175$ C km and (b) a strong discharge $hQ_{max} = 560$ C km causing halo. The total accumulated charge in the lower ionosphere at 10 ms calculated by spatial integration is (Figure 3a) $Q_i = -2.56$ C and (Figure 3b) $Q_i = -8.15$ C. (c) We plot the difference between E/Q_{max} at ground level for two different discharges at different times. We can see the halo influence in the first kilometers causing a sign change in the difference.

2. *Changes in the electron density due to the chemical scheme* (3). A higher electron density accelerates screening and lowers the ionosphere's edge, whereas a lower electron density slows down the screening. Referring again to our previous arguments, this implies that ionization decreases E/Q_{max} whereas attachment increases this ratio.

In Figure 3c we compare the ratios E/Q_{max} from our model discharges for a range of distances and at several times. Initially, the effect of the field-dependent mobility dominates, and the field is relatively smaller for the weak discharge. However, as ionization lowers down the edge of the ionosphere we see that at short distances the field becomes relatively weaker for the strong discharge, as we argued above. Far from the discharge the electric fields in the ionosphere are not strong enough for ionization, so the effects of attachment and field-dependent mobilities dominate; so E/Q_{max} is higher for the strong discharge. Note, however, that these nonlinear effects are extremely small, amounting to less than 3% of the total field. This effect is therefore probably undetectable.

5. Conclusions

We have argued that the activity of a halo cannot explain, or at least cannot explain in a straightforward manner, an enhancement in the distant electrostatic field created by a lightning stroke. We therefore believe that some other explanation is needed for the observations of *Bennett and Harrison* [2013]. At present we do not have a satisfactory alternative, but we conclude this letter by listing and discussing some issues that are missing in our models and may provide a path for future investigations.

One such issue is the DC voltage bias between the ground and the ionosphere. Assuming that the electric field caused by this potential difference is uniform, a decrease of the ionosphere's altitude, say, from 90 km to 70 km, enhances the fair-weather electric field by a factor $90/70 \approx 1.3$, that is, 30%. This is a wide upper limit for the increase since the atmospheric conductivity increases exponentially with altitude and the potential difference is located at low altitude. However, even the 30% figure looks too small to account for the observed features.

A second issue is the presence of other sources of ionization in the space between the cloud tops and the ionosphere. As electric fields high enough to cause ionization are also capable of inducing light emissions,

the source of ionization that we seek must also be a type of TLE. Due to their rarity, we can dismiss jets and giant blue jets. We have sprites and elves as remaining candidates.

Sprites are certainly associated with intense ionization. To investigate their effects, we run simulations where a sprite is modeled as a large, elliptical cloud of ionization above the discharge. The resulting electrostatic field at ground level is barely distinguishable from the field without a sprite, although slightly smaller. However, we considered only cases with cylindrical symmetry and therefore did not investigate sprites with a footprint of tens of kilometers away from the causative discharge as is often the case [*Vadislavsky et al.*, 2009].

The electromagnetic pulse (EMP) emitted by the lightning stroke, visible as an elve as it reaches the lower ionosphere, may also cause significant ionization. Although usually this ionization increases the conductivity by only a few percent [*Marshall*, 2012], in certain extreme cases the increase may be much higher [*Gordillo-Vázquez et al.*, 2016]. The highest-energy deposition by an EMP interacting with the ionosphere is at a propagation angle of about 45° [*Luque et al.*, 2014], i.e., at a distance of about 9 km from the vertical axis containing the causative stroke. Due to the curvature effect that we discussed above, the ionization caused by the EMP may possibly increase the electrostatic field at ground level at about this distance. However, we consider EMP-driven ionization as an unlikely explanation for the observations of *Bennett and Harrison* [2013]: it requires too many intense EMPs and cannot account for any polarity reversal.

Detailed time-resolved and wide-band measurements would greatly illuminate the physics behind the polarity reversal and the violation of the cubic law measured by *Bennett and Harrison* [2013]. This would clarify whether electrostatic fields are a viable alternative for the remote detection and characterization of electric storms.

Acknowledgments
This work was supported by the Spanish Ministry of Science and Innovation, MINECO under projects ESP2013-48032-C5-5-R, FIS2014-61774-EXP, and ESP2015-69909-C5-2-R and by the EU through the FEDER program. F.J.P.I. acknowledges a MINECO predoctoral contract, code BES-2014-069567. A.L. acknowledges support by a Ramón y Cajal contract, code RYC-2011-07801. All data used in this paper are directly available after a request is made to authors F.J.P.I. (fjpi@iaa.es), A.L. (aluque@iaa.es) or F.J.G.V. (vazquez@iaa.es).

References

Barrington-Leigh, C. P., U. S. Inan, and M. Stanley (2001), Identification of sprites and elves with intensified video and broadband array photometry, *J. Geophys. Res.*, *106*, 1741–1750, doi:10.1029/2000JA000073.

Bennett, A. J. (2014), Modification of lightning quasi-electrostatic signal by mesospheric halo generation, *J. Atmos. Sol. Terr. Phys.*, *113*, 39–43, doi:10.1016/j.jastp.2014.03.010.

Bennett, A. J., and R. G. Harrison (2013), Lightning-induced extensive charge sheets provide long range electrostatic thunderstorm detection, *Phys. Rev. Lett.*, *111*(4), 045003, doi:10.1103/PhysRevLett.111.045003.

Betz, H. D., K. Schmidt, P. Laroche, P. Blanchet, W. P. Oettinger, E. Defer, Z. Dziewit, and J. Konarski (2009), LINET — An international lightning detection network in Europe, *Atmos. Res.*, *91*, 564–573, doi:10.1016/j.atmosres.2008.06.012.

Borwein, J., M. Glasser, R. McPhedran, J. Wan, and I. Zucker (2013), *Lattice Sums Then and Now, Encycl. of Math. and its Appl.*, Cambridge Univ. Press, Cambridge, U. K.

Cummins, K. L., and M. J. Murphy (2009), An overview of lightning locating systems: History, techniques, and data uses, with an in-depth look at the U.S. NLDN, *IEEE Trans. Electromag. Compat.*, *51*(3), 499–518, doi:10.1002/2015JA021408.

Cummins, K. L., M. J. Murphy, E. A. Bardo, W. L. Hiscox, R. B. Pyle, and A. E. Pifer (1998), A combined TOA/MDF technology upgrade of the U.S. National Lightning Detection Network, *J. Geophys. Res.*, *103*, 9035–9044, doi:10.1029/98JD00153.

Dowden, R. L., J. B. Brundell, and C. J. Rodger (2002), VLF lightning location by time of group arrival (TOGA) at multiple sites, *J. Atmos. Sol. Terr. Phys.*, *64*, 817–830, doi:10.1016/S1364-6826(02)00085-8.

Ebert, U., S. Nijdam, C. Li, A. Luque, T. Briels, and E. van Veldhuizen (2010), Review of recent results on streamer discharges and discussion of their relevance for sprites and lightning, *J. Geophys. Res.*, *115*, A00E43, doi:10.1029/2009JA014867.

Franz, R. C., R. J. Nemzek, and J. R. Winckler (1990), Television image of a large upward electrical discharge above a thunderstorm system, *Science*, *249*, 48–51, doi:10.1126/science.249.4964.48.

Gordillo-Vázquez, F. J., A. Luque, and C. Haldoupis (2016), Upper *D* region chemical kinetic modeling of lore relaxation times, *J. Geophys. Res. Space Physics*, *121*, 3525–3544, doi:10.1002/2015JA021408.

Hagelaar, G. J. M., and L. C. Pitchford (2005), Solving the Boltzmann equation to obtain electron transport coefficients and rate coefficients for fluid models, *Plasma Sources Sci. Technol.*, *14*, 722–733, doi:10.1088/0963-0252/14/4/011.

Hu, W., S. A. Cummer, and W. A. Lyons (2007), Testing sprite initiation theory using lightning measurements and modeled electromagnetic fields, *J. Geophys. Res.*, *112*, D13115, doi:10.1029/2006JD007939.

Kuo, C. L., et al. (2013), Ionization emissions associated with N_2^+ 1N band in halos without visible sprite streamers, *J. Geophys. Res. Space Physics*, *118*, 5317–5326, doi:10.1002/jgra.50470.

Lawton, S. A., and A. V. Phelps (1978), Excitation of the $b\ ^1\Sigma^+_g$ state of O_2 by low energy electrons, *J. Chem. Phys.*, *69*, 1055, doi:10.1063/1.436700.

Liu, N. (2012), Multiple ion species fluid modeling of sprite halos and the role of electron detachment of O^- in their dynamics, *J. Geophys. Res.*, *117*, A03308, doi:10.1029/2011JA017062.

Liu, N., J. R. Dwyer, H. C. Stenbaek-Nielsen, and M. G. McHarg (2015a), Sprite streamer initiation from natural mesospheric structures, *Nat. Commun.*, *6*, 7540, doi:10.1038/ncomms8540.

Liu, N., M. G. McHarg, and H. C. Stenbaek-Nielsen (2015b), High-altitude electrical discharges associated with thunderstorms and lightning, *J. Atmos. Sol. Terr. Phys.*, *136*, 98–118, doi:10.1016/j.jastp.2015.05.013.

Liu, N., N. Spiva, J. R. Dwyer, H. K. Rassoul, D. Free, and S. A. Cummer (2015c), Upward electrical discharges observed above Tropical Depression Dorian, *Nat. Commun.*, *6*, 5995, doi:10.1038/ncomms6995.

Luque, A., and U. Ebert (2009), Emergence of sprite streamers from screening-ionization waves in the lower ionosphere, *Nat. Geosci.*, *2*, 757–760, doi:10.1038/ngeo662.

Luque, A., and U. Ebert (2012), Density models for streamer discharges: Beyond cylindrical symmetry and homogeneous media, *J. Comput. Phys.*, *231*, 904–918, doi:10.1016/j.jcp.2011.04.019.

Luque, A., and F. J. Gordillo-Vázquez (2012), Mesospheric electric breakdown and delayed sprite ignition caused by electron detachment, *Nat. Geosci.*, *5*, 22–25, doi:10.1038/ngeo1314.

Luque, A., D. Dubrovin, F. J. Gordillo-Vázquez, U. Ebert, F. C. Parra-Rojas, Y. Yair, and C. Price (2014), Coupling between atmospheric layers in gaseous giant planets due to lightning-generated electromagnetic pulses, *J. Geophys. Res. Space Physics*, *119*, 8705–8720, doi:10.1002/2014JA020457.

Maggio, C. R., T. C. Marshall, and M. Stolzenburg (2009), Estimations of charge transferred and energy released by lightning flashes, *J. Geophys. Res.*, *114*, D14203, doi:10.1029/2008JD011506.

Marshall, R. A. (2012), An improved model of the lightning electromagnetic field interaction with the *D*-region ionosphere, *J. Geophys. Res.*, *117*, A03316, doi:10.1029/2011JA017408.

Neubert, T., O. Chanrion, E. Arnone, F. Zanotti, S. Cummer, J. Li, M. Füllekrug, S. Soula, and O. van der Velde (2011), The properties of a gigantic jet reflected in a simultaneous sprite: Observations interpreted by a model, *J. Geophys. Res.*, *116*, A12329, doi:10.1029/2011JA016928.

Parra-Rojas, F. C., A. Luque, and F. J. Gordillo-Vázquez (2013), Chemical and electrical impact of lightning on the Earth mesosphere: The case of sprite halos, *J. Geophys. Res. Space Physics*, *118*, 5190–5214, doi:10.1002/jgra.50449.

Pasko, V. P. (2010), Recent advances in theory of transient luminous events, *J. Geophys. Res.*, *115*, A00E35, doi:10.1029/2009JA014860.

Pasko, V. P., Y. Yair, and C.-L. Kuo (2012), Lightning related transient luminous events at high altitude in the Earth's atmosphere: Phenomenology, mechanisms and effects, *Space Sci. Rev.*, *168*, 475–516, doi:10.1007/s11214-011-9813-9.

Phelps, A. V., and L. C. Pitchford (1985), Anisotropic scattering of electrons by N2 and its effect on electron transport, *Phys. Rev. A*, *31*, 2932–2949, doi:10.1103/PhysRevA.31.2932.

Qin, J., V. P. Pasko, M. G. McHarg, and H. C. Stenbaek-Nielsen (2014), Plasma irregularities in the *D*-region ionosphere in association with sprite streamer initiation, *Nat. Commun.*, *5*, 3740, doi:10.1038/ncomms4740.

Rakov, V. A. (2013), Electromagnetic methods of lightning detection, *Surv. Geophys.*, *34*, 731–753, doi:10.1007/s10712-013-9251-1.

Rayment, S., and J. Moruzzi (1978), Electron detachment studies between O^- ions and nitrogen, *Int. J. Mass Spectrom. Ion Phys.*, *26*(3), 321–326, doi:10.1016/0020-7381(78)80033-3.

Rycroft, M. J., S. Israelsson, and C. Price (2000), The global atmospheric electric circuit, solar activity and climate change, *J. Atmos. Sol. Terr. Phys.*, *62*, 1563–1576, doi:10.1016/S1364-6826(00)00112-7.

United States Committee on Extension to the Standard Atmosphere (1976), U.S. Standard Atmosphere, National Oceanic and Amospheric [sic] Administration : for sale by the Supt. of Docs., U.S. Govt. Print. Off.

Vadislavsky, E., Y. Yair, C. Erlick, C. Price, E. Greenberg, R. Yaniv, B. Ziv, N. Reicher, and A. Devir (2009), Indication for circular organization of column sprite elements associated with eastern Mediterranean winter thunderstorms, *J. Atmos. Sol. Terr. Phys.*, *71*, 1835–1839, doi:10.1016/j.jastp.2009.07.001.